Supplementary Information

Efficient Visible Light-Driven Water Oxidation and Proton Reduction by an Ordered Covalent Triazine-Based Framework

Jijia Xie,[a] Stephen A. Shevlin,[b] Qiushi Ruan,[a] Savio J. A. Moniz,[a] Yangrong Liu,[b] Xu Liu,[a] Yaomin Li,[b] Chi Ching Lau,[a] Zheng Xiao Guo,[b] and Junwang Tang*[a]*

Material preparation

CTF-1s was prepared as mentioned in the Experimental section. The time-on-line synthesis temperature profiles for each sample are shown in Figure S1. 20W and 50W microwave irradiation powers show similar trends of temperature, which almost linearly increases from room temperature to *ca.* 55°C. When increasing the microwave power to 100W, the temperature reaches 120 °C after 30 seconds microwave irradiation. Further enhancing the power to 200W, the temperature first increases to 55°C and then the microwave power is interrupted due to the pressure higher than the regulated safety value as shown in Figure S2. The temperature finally reaches 120°C after 30 seconds in the study.

The pressure profiles are shown in Figure S2. There is not evident pressure change during 30-second 20W microwave irradiation. When increasing the microwave power to 50W, the final pressure reaches *ca.* 40 psi after 30 seconds. Further enhance the power to 100W, the pressure increases to the regulated safety value of 200 psi in 25 seconds, and then the power is interrupted and the pressure further increases to *ca.* 340 psi. When irradiating the reactor by 200W microwave power, the pressure rapidly raises to 200 psi in 8 seconds. Then, the power is interrupted as mentioned above and finally keeps at *ca.* 300 psi.

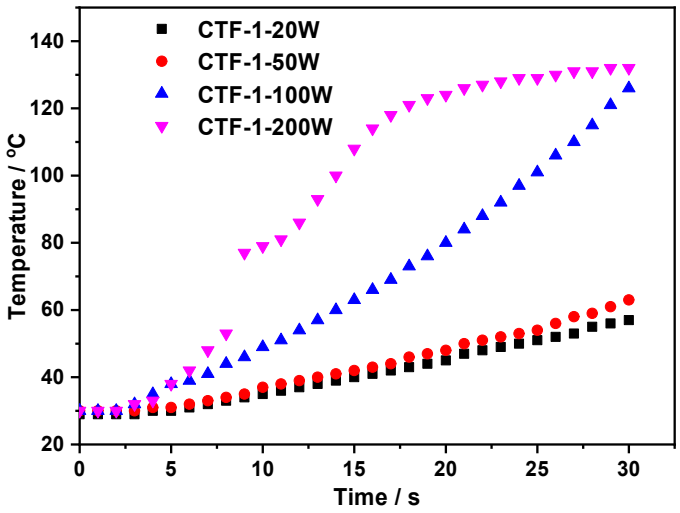

Figure S1 Time-on-line synthesis temperature profile of CTF-1s during microwave irradiation.

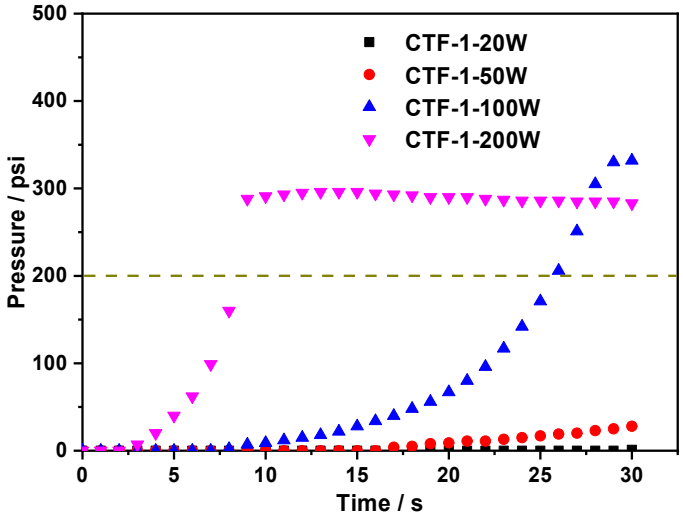

Figure S2 Time-on-line synthesis pressure profile of CTF-1s during microwave irradiation.

FT-IR Before and after OER

FT-IR spectra were utilised to prove the stability of material structure before and after 18-hour OER under visible light irradiation. The additional very broad but shallow peak at *ca.* 3000-3500 cm^{-1} is associated with the remaining water in the water splitting reaction.

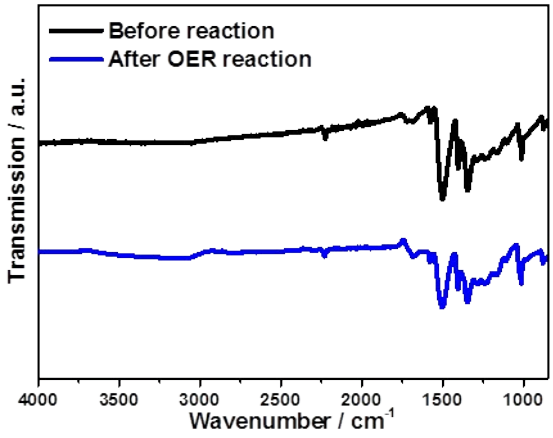

Figure S3 FT-IR spectra of CTF-1 before and after 18 h of OER reaction.

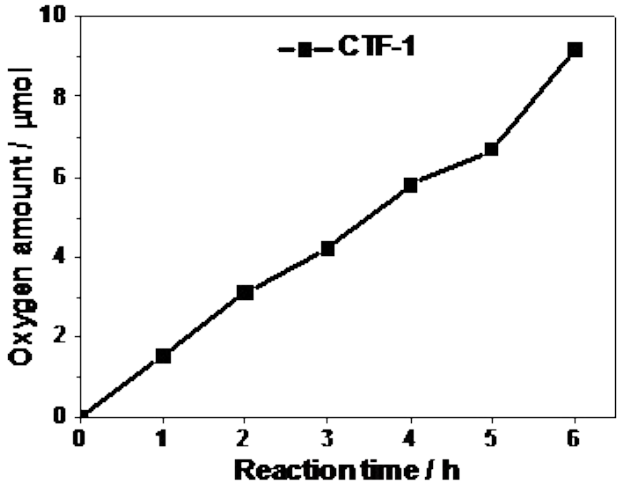

Figure S4 . Oxygen production from water using 50mg CTF-1-100W containing 0.05M AgNO3 as electron scavenger under visible irradiation (λ ≥420nm) for 6 h.

Characterisation of RuO_x/CTF-1-100W

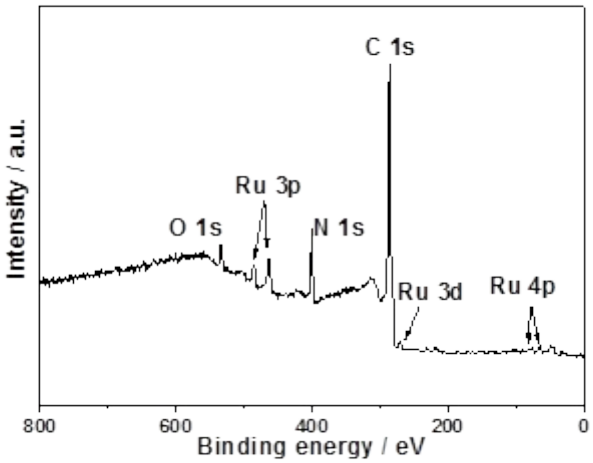

Figure S5 XPS survey spectrum of RuO/CTF-1-100W.

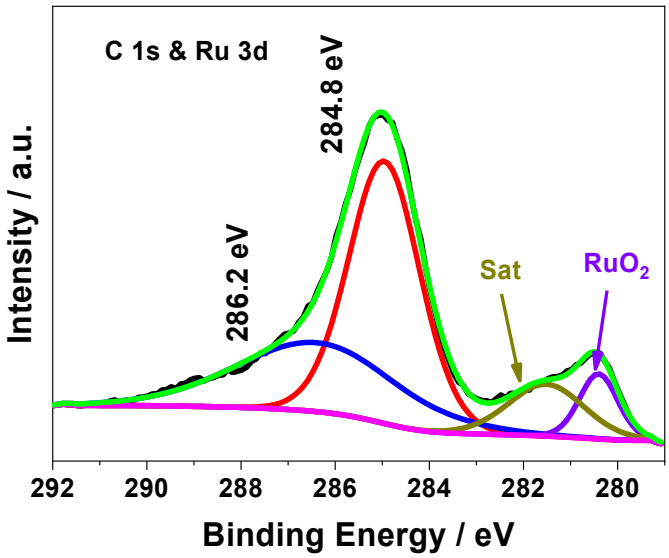

Figure S6 C1s and Ru 3d XPS spectrum of RuO/CTF-1-100W.

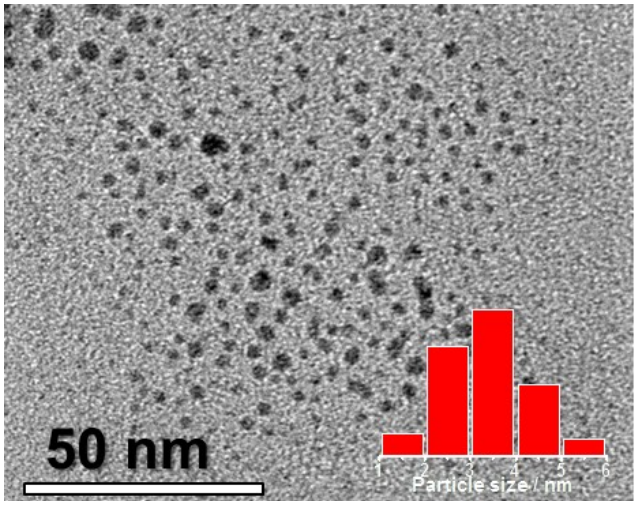

Figure S7 TEM image of RuO/CTF-1-100W.

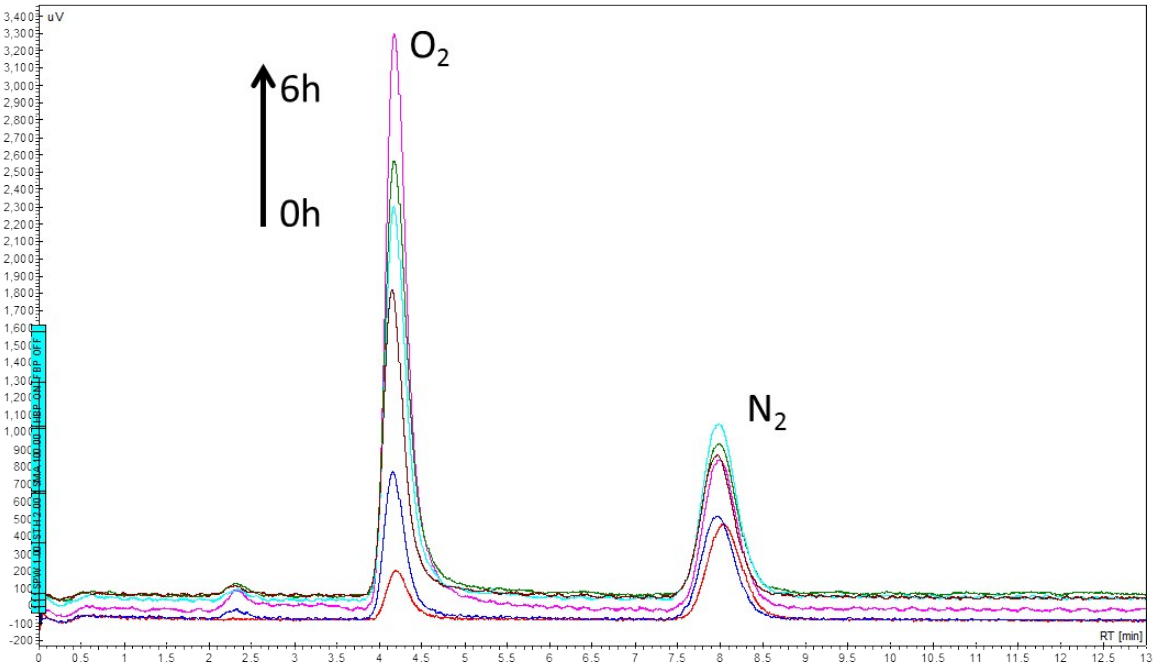

Figure S8 Gas chromatography spectrum during typecal run in the of OER as shown in Figure 4a.

Characterisation of Pt/CTF-1-100W

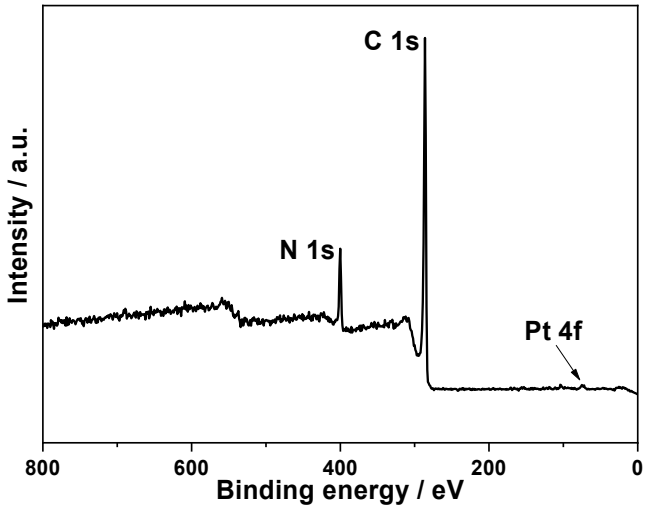

Figure S9 XPS survey spectrum of Pt/CTF-1-100W.

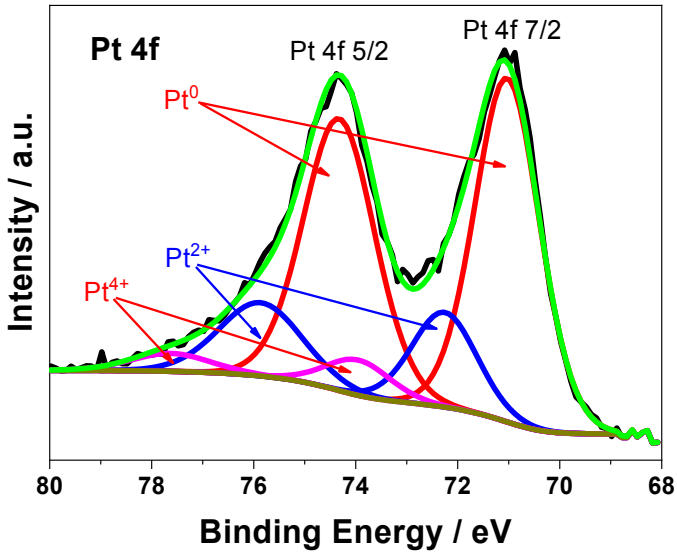

Figure S10 Pt 4f XPS spectrum of Pt/CTF-1-100W.

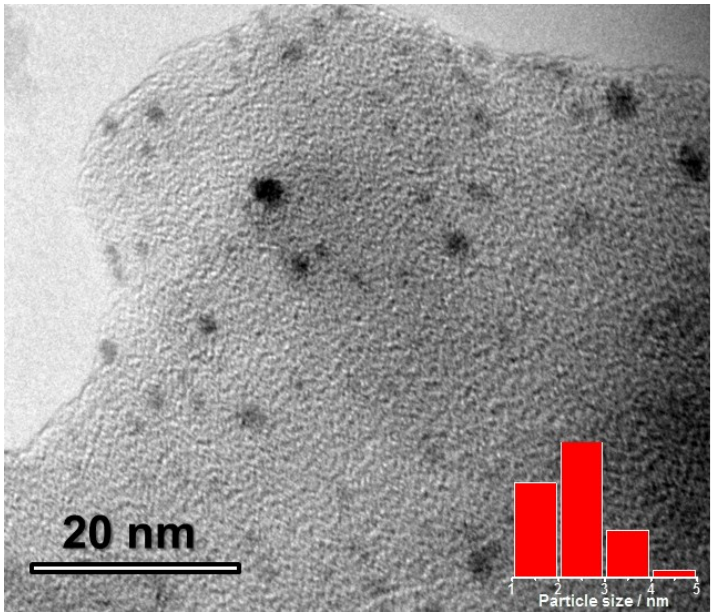

Figure S11 TEM image of Pt/CTF-100W.

g-C_3N_4 as a reference photocatalyst was prepared according to the literature.[1] Briefly, Urea (Sigma-Aldrich, 99%) was placed in a high quality alumina crucible with lid, then placed inside a muffle furnace and heated at a ramp rate of 5 ^{o}C/minute and finally held at 600 °C for four hours. The resultant powders were then washed with water, HCl, NaOH and once again with water to remove all unreacted precursor and impurities. XPS, FT-IR and UV-Vis spectra were carried out to check the quality of the synthesised material, and showed similar results with those reported (see Figure S15 and S16).

Fitting of percentage of exact exchange to bandgap

We altered the percentage of exact exchange in order to match experimental values for the bulk bandgaps of the two materials, 2.7 eV for g-C_3N_4,[2] and 2.5 eV for CTF-1, as shown in Figure S6. We also found that to match the experimental bandgap of g-C_3N_4 18.12% exact exchange is needed, while to match the experimental bandgap of CTF-1 5.00% exact exchange is needed. Using these values we found that both sheets exhibit quantum size effects, 0.105 eV for *g*-C_3N_4 and 0.426 eV for CTF-1. The low percentage of exact exchange required to match the experimental bandgap, and the

significant quantum size effect for the single sheet indicate that CTF-1 possesses far more delocalisation of the conduction and valence band edges.

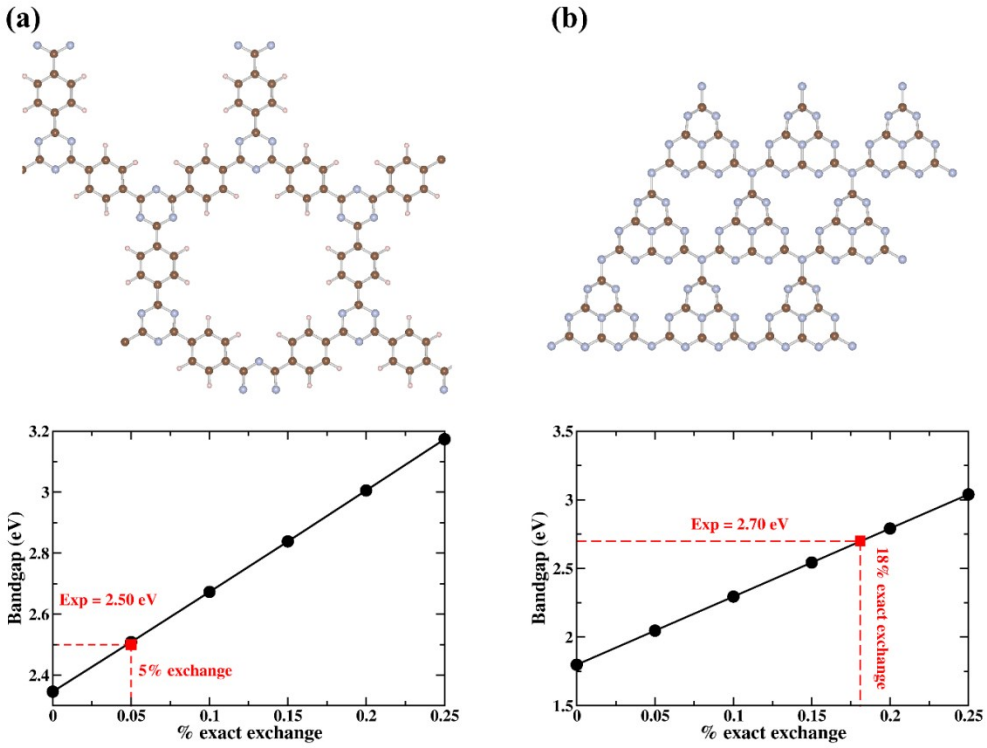

Figure S12 Structure and fitting of exact exchange to experimental bandgap for (a) CTF-1, and (b) *g*-C_3N_4.

Table S1 Representative summary of the photocatalytic activity of covelent triazine-based photocatalysts toward water splitting and selected modified C_3N_4 published in 2017-2018.

Materials	Synthesis Parameters	HER activity[a] (μmol h^{-1})	HER AQY (%)	OER activity[b] (μmol h^{-1})	OER AQY(%)	Ref.
TFPT-COF	120 °C, 72h	19.7	-	-	-	[3] 2014
CTF-1	400°C, 46h	0.02	-	no oxygen detected	-	[4] 2015
PTO-300-15	300 °C, 168h	9	5.5± 1.1 (400±20nm)	no oxygen detected	-	[4] 2015
N_3-COF	120 °C, 72h	8.51	0.15 (400nm)	-	-	[5] 2015
CTF-T1	25 °C, 72h	2	2.4 (400-440nm)	0.15	-	[6] 2015
$CTFS_x$	250 °C 1h, then 60 °C 12h	80	-	-	-	[7] 2016
CTF-1_10min	40°C 48h, then 400 °C 10min	26.8	6.4 (450 ± 10nm)	-	-	[8] 2017
CTF-HUST-2	60-100 °C, 24h	150	-	-	-	[9] 2017
CTP-2	0 °C, 1h, 100 °C, 20min	28	-	1.5	-	[10] 2017
CTF-1-100W	<200 °C, 30s	264.86	6.0 (420nm)	6.97	3.8(420nm)	This work
$Pt/CNPS-NH_2$	Modified C_3N_4	-	-	120	-	[11] 2018
Pt/CNLH-600		-	-	10	10.3(420nm)	[12] 2017
Pt/CN aerogels		-	-	30	3.1(420nm)	[13] 2017
Pt/CCNNSs		-	-	55	8.57 (420nm)	[14] 2017

a: Hydrogen evolution reaction (HER) activity under visible light (>420 nm)

b: Oxygen evolution reaction (OER) activity under visible light (>420 nm)

XPS before and after OER and HER

Figure S13 shows the XPS before and after the 3-day oxygen and hydrogen evolution reactions which were conducted under visible light irradiation. As shown in Figure S13 a, the Carbon 1s peak is found at around 286 eV and the small peak at 400 eV is assigned to N 1s. However, the carbon peak is much larger than the nitrogen peak, which is due to the adventitious carbon used for calibration.[10]

Elemental analysis (EA) gives a more precise carbon to nitrogen ratio, where the carbon, nitrogen and hydrogen ratio is 75.3 wt. CARBON %, 21.0 wt. NITROGEN % and 3.7 wt. HYDROGEN %, respectively. Figure S13b and S13c give more detail of the chemical and electronic states of the carbon and nitrogen atoms, which can further support the results gained by FT-IR and ssNMR. The C1s spectrum of CTF-1 contains two contributions with binding energies at 284.8 eV and 286.2 eV, which are associated with the carbon atom in phenyl (or calibration carbon) and triazine (or nitrile) ring, respectively. The N1s spectrum can be de-convoluted into two peaks at 398.9 eV and 400.2 eV, which corresponds to the nitrogen atom in the triazine rings and the uncondensed nitrile groups, respectively.[10] Figure S13e reveals that the Ru co-catalyst predominantly exists in the form of $RuO_2 \cdot xH_2O$.[11]

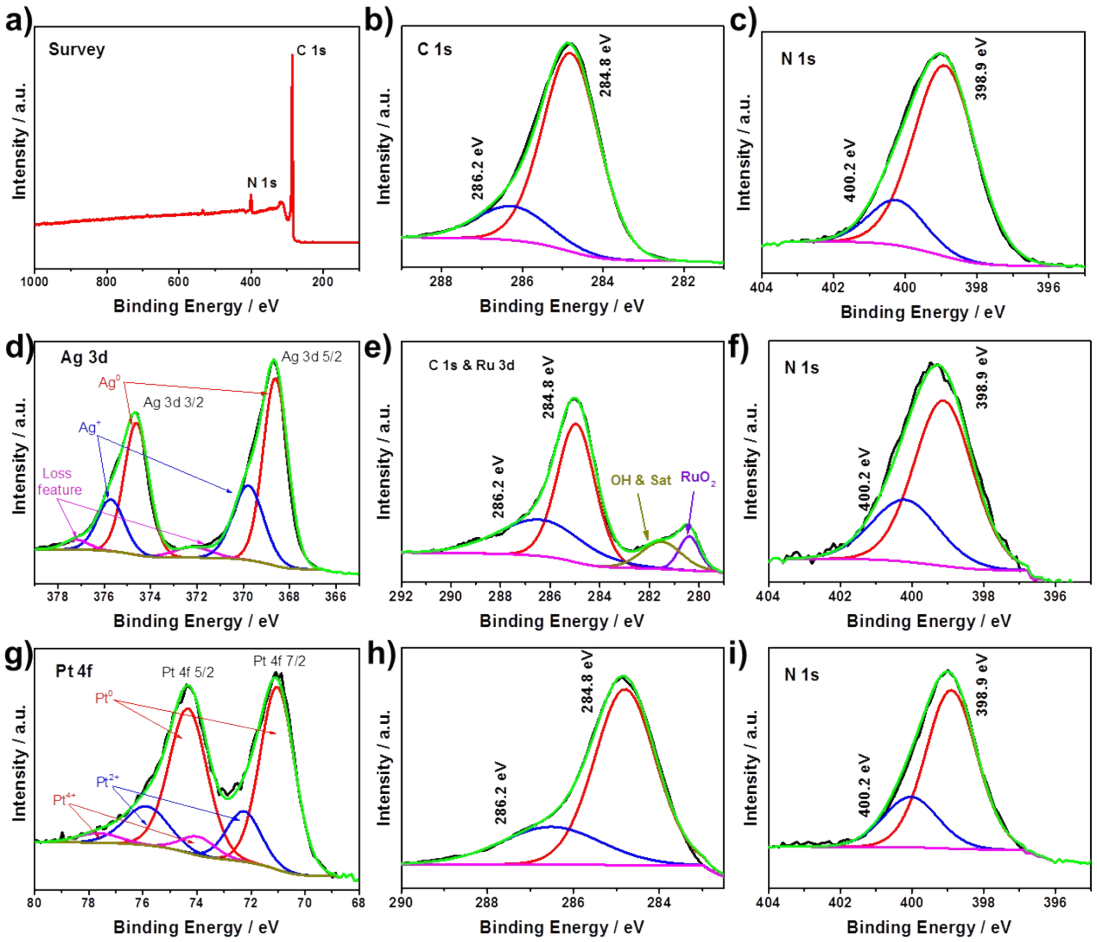

Figure S13 XPS spectra (a) Survey, (b) C 1s, (c) N 1s before reaction; (d) Ag 3d, (e) C 1s & Ru 3d (f) N 1s after oxygen evolution reaction and (g) Pt 4f, (h) C1s, (i) N1s after hydrogen evolution reaction.

Raman spectra before and after OER and HER

Raman spectra was used to prove the stability of the conjugated structure before and after 18-hour OER and HER testing under visible light irradiation, respectively.

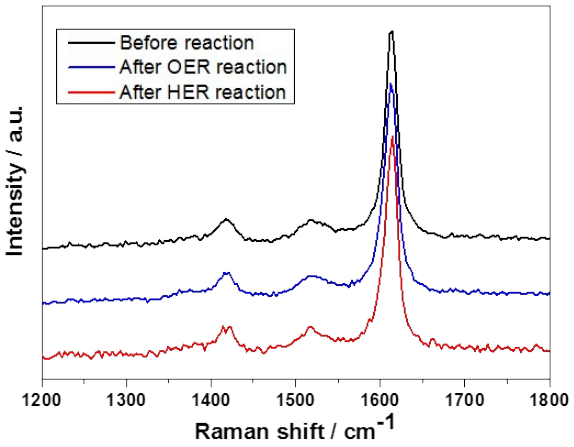

Figure S14 Raman spectra of CTF-1 before and after photocatalytic reactions.

g-C_3N_4 characterisation

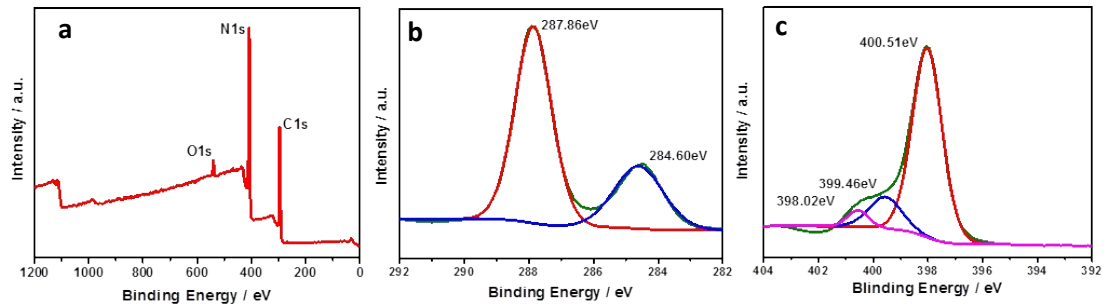

Figure S15 XPS spectra of g-C_3N_4 (a) Survey (b) C1s and (c) N1s.

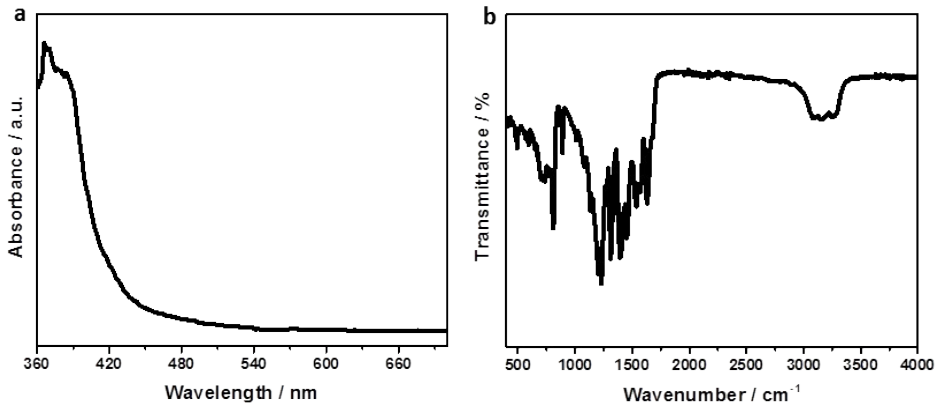

Figure S16 (a) UV-Vis and (b) FT-IR spectra of g-C_3N_4

References

1 D. Martin, K. Qiu, S. Shevlin, A. Handoko, X. Chen, Z. Guo and J. Tang, *Angew. Chemie Int. Ed.*, 2014, **53**, 9240–9245.

2 X. Wang, K. Maeda, A. Thomas, K. Takanabe, G. Xin, J. M. Carlsson, K. Domen and M. Antonietti, *Nat. Mater.*, 2009, **8**, 76–80.

3 L. Stegbauer, K. Schwinghammer and B. V. Lotsch, *Chem. Sci.*, 2014, **5**, 2789–2793.

4 K. Schwinghammer, S. Hug, M. B. Mesch, J. Senker and B. V. Lotsch, *Energy Environ. Sci.*, 2015, **8**, 3345–3353.

5 V. S. Vyas, F. Haase, L. Stegbauer, G. Savasci, F. Podjaski, C. Ochsenfeld and B. V. Lotsch, *Nat. Commun.*, 2015, **6**, 8508.

6 J. Bi, W. Fang, L. Li, J. Wang, S. Liang, Y. He, M. Liu and L. Wu, *Macromol. Rapid Commun.*, 2015, **36**, 1799–1805.

7 L. Li, W. Fang, P. Zhang, J. Bi, Y. He, J. Wang and W. Su, *J. Mater. Chem. A*, 2016, **4**, 12402–

12406.

8 S. Kuecken, A. Acharjya, L. Zhi, M. Schwarze, R. Schomäcker and A. Thomas, *Chem. Commun.*, 2017, **53**, 5854–5857.

9 K. Wang, L. M. Yang, X. Wang, L. Guo, G. Cheng, C. Zhang, S. Jin, B. Tan and A. Cooper, *Angew. Chemie Int. Ed.*, 2017, **56**, 14149–14153.

10 Z. A. Lan, Y. Fang, Y. Zhang and X. Wang, *Angew. Chemie Int. Ed.*, 2018, **57**, 470–474.

11 N. Meng, J. Ren, Y. Liu, Y. Huang, T. Petit and B. Zhang, *Energy Environ. Sci.*, 2018, **11**, 566–571.

12 Y. Wang, M. K. Bayazit, S. J. A. Moniz, Q. Ruan, C. C. Lau, N. Martsinovich and J. Tang, *Energy Environ. Sci.*, 2017, **10**, 1643–1651.

13 H. Ou, P. Yang, L. Lin, M. Anpo and X. Wang, *Angew. Chemie Int. Ed.*, 2017, **56**, 10905–10910.

14 H. Ou, L. Lin, Y. Zheng, P. Yang, Y. Fang and X. Wang, *Adv. Mater.*, 2017, **29**, 1700008.